22

Myoelectric Knee Angle Estimation Algorithms for Control of Active Transfemoral Leg Prostheses

Alberto L. Delis[1,2], Joao L. A. Carvalho[1], Adson F. da Rocha[1],
Francisco A. O. Nascimento[1] and Geovany A. Borges[1]
[1]*Department of Electrical Engineering, University of Brasilia, Brasilia-DF*
[2]*Medical Biophysics Center, University of Oriente, Santiago de Cuba*
[1]*Brazil*
[2]*Cuba*

1. Introduction

The electromyographic signal is the electrical manifestation of the neuromuscular activation associated with a contracting muscle. The surface electromyographic (SEMG) signal represents the current generated by ionic flow across the membrane of the muscle fibers that propagates through the intervening tissues to reach the detection surface of an electrode located over skin (De Luca (2006)). The SEMG signal provides a non-invasive tool for investigating the properties of skeletal muscles (Sommerich et al. (2000)). The main challenge in implementing controlled motion for prosthesis is correctly predicting the user's motion intention. SEMG signals have been used in an effective way in prosthesis control systems (Merletti & Parker (2004); Parker et al. (2006)). The SEMG signal is very convenient for prosthesis control, because it is intrinsically related to the user's intention (Hudgins et al. (1993)). A myoelectric control algorithm should be capable of learning the muscular activation patterns that are used in natural form for typical movements. It also needs robustness against variations in conditions during the operation, and the response time cannot create delays that are noticeable to the user (Fukuda et al. (2003)). Pattern recognition of the SEMG signal allows discriminating amongst the desired classes of limb motion and plays a key role in advanced control of powered prostheses for amputees and for individuals with congenital deficiency in the upper or lower limbs. The success of a myoelectric control scheme depends greatly on the classification accuracy.

Electronic knees can be designed for providing different levels of damping during swing, and for adjusting to different walking speeds, assuming they have the appropriate sensors and control algorithms for estimating the knee joint angle and the walking speed. With the appropriate control algorithm, it is possible to program the prosthesis to allow the knee to flex and extend while bearing a subject's weight (stance flexion). This feature of normal walking is not possible with conventional prostheses. Electronic knees use some form of computational intelligence to control the resistive torque about the knee. Several research groups have been involved in designing prototype knee controllers. Grimes et al. (1977) developed an echo control scheme for gait control, in which a modified knee trajectory from the sound leg is played back on the contralateral side. Popovic et al. (1995) presented a battery-powered active knee joint actuated by direct-current motors, together with a finite state knee controller

that utilizes a robust position tracking control algorithm for gait control. A small number of companies have also developed electronic knees for clinical use. For example, the Otto Bock C-leg (Kastner et al. (1999)) provides adjustable resistance for flexion and extension in swing through onboard intelligence and a special software package. Figure 1 presents the ongoing development of an active leg prosthesis prototype. The prosthesis has three degrees of freedom: one for the knee (sagittal plane), and two movements for the foot (sagittal and frontal plane). The three degrees of freedom are controlled by direct-current reduction motors. Onboard sensors allow estimating the foot orientation with respect to the ground (Ishihara et al. (2009)). This allows the foot to be oriented according to the terrain.

A pattern-recognition-based myoelectric control algorithm is typically composed of various main modules; a data segmentation stage handles the data before feature extraction, to improve precision and response time. A feature extraction stage pre-processes the data for reducing the amount of information to be analyzed. New variables (features) may be obtained by linear or non-linear transformation of the original data. The central component is the neural network classifier, which must be capable of learning relations between the input features and the desired control outputs. Significant advancements in pattern recognition methodology are in progress. A common approach is to extract parameters from the data, such as time-domain features (e.g., mean absolute value, waveform length, number of zero crossings) (Kelly et al. (1990); Hudgins et al. (1993)), spectral parameters (e.g., auto-regressive model) (Huang et al. (2005);Hargrove et al. (2008)), time-frequency coefficients (e.g., short-time Fourier transform) (Englehart et al. (2001)), and/or time-scale coefficients (e.g., discrete wavelet transform, wavelet packet decomposition) (Englehart et al. (2001); Chu et al. (2005); Wang et al. (2006)). Further data reduction may be achieved using a feature projection stage between pre-processing and classification (Englehart et al. (2001); Chu et al. (2005); Wang et al. (2006)). This approach eliminates redundant information, which speeds up the training process. It may also help mapping the data into small and well-separated clusters, by absorbing signal variations and noise present in the data's original vector-space.

The data processing and classification techniques discussed above have been successfully used for myoelectric control by several groups. Kelly et al. (1990) proposed an algorithm capable of discriminating between four motions of elbow and wrist joints from SEMG patterns measured from one pair of electrodes, using a Hopfield neural network for time-domain feature extraction, followed by a two-layer perceptron neural classifier. Englehart et al. (2001) designed an algorithm for dexterous and natural myoelectric control of powered upper limbs using a linear discriminant analysis (LDA) classifier, after principal component analysis (PCA) dimensionality reduction on a wavelet-based feature set. Chu et al. (2005) presented a pattern recognition algorithm for the control of a multifunction myoelectric hand, using the wavelet packet transform for feature extraction, a multilayer neural network classifier, and a linear-nonlinear feature projection composed of PCA and self-organizing feature maps, respectively. Huang et al. (2005) designed a classification scheme based on Gaussian mixture models for myoelectric control of upper limb prostheses, using feature extraction based on time-domain statistics, auto-regressive (AR) coefficients, and the root mean square of the signal. Wang et al. (2006) proposed an algorithm capable of discriminating between four types of hand and forearm movements, using wavelet packet feature extraction and PCA feature projection. Zhao et al. (2006) designed a control algorithm capable of recognizing six different hand motion patterns, using a multi-layer perceptron neural network classifier and feature extraction based on sample entropy, time-domain filtering, and wavelet transform coefficients. Hargrove et al. (2008) used a combination of time-domain features and AR coefficients with

a LDA classifier to determine the effect of electrode displacements on pattern classification accuracy, and to design a classifier training strategy to address this issue.

The application of multisensor data fusion has found widespread use in diverse areas (industry, commerce, local robot guidance for global military defense, etc.) (Luo et al. (2002)). Data fusion is the continuous process of implementing a model of the domain of interest, utilizing data of different natures (Gao & Harris (2002)). The purpose of data fusion is to produce an improved model or estimate of a system from a set of independent data sources. The use of range sensory data allows automatic extraction of information about the sensed environment under different operating conditions, and increases the performance, reliability, data rates and autonomy of the system (Luo (1996);Hall & Llinas (1997);Dasarathy (1997)). In many real-time applications, the desired model is the state vector of the dynamic process (Ferreira et al. (2005);Delis et al. (2009a)). The combination of the information from the sensors and subsequent estimation of the state should be done in a coherent manner, such that the uncertainty is reduced. The Kalman filter is a state estimator algorithm widely used for optimally estimating the unknown state of a linear dynamic system from Gaussian distributed noisy observations (Manyika & Durrant-Whyte (1994)). The algorithm uses a predefined model of the system to predict the state at the next time step (Diniz (1997)). The fusion of SEMG signals with other data is not common in the literature.

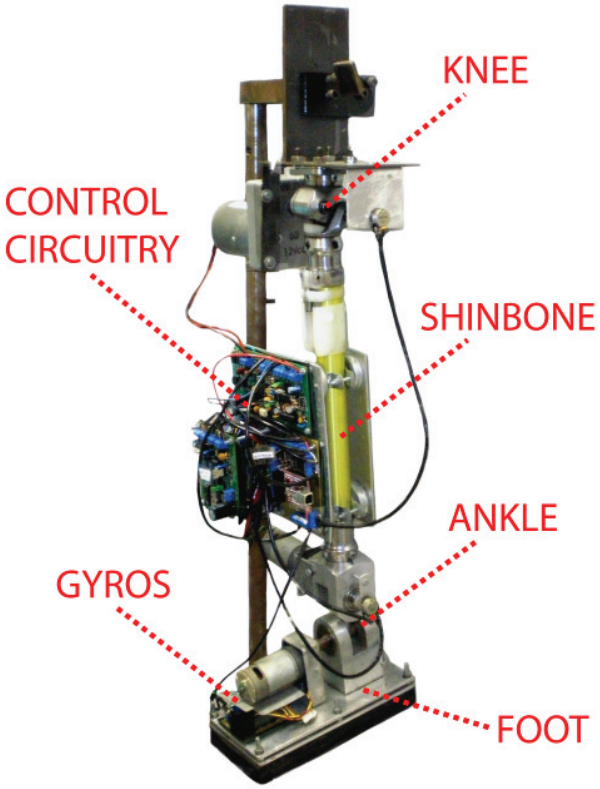

Fig. 1. Prototype of a leg prosthesis for transfemoral amputees.

Silva et al. (2003) applied data fusion of mechanomyography signals for the generation of binary control signals for an electrically powered prosthesis. The goal was to implement a practical mechanomyography-based detection system of muscle contractions for prosthesis control. Silicon-embedded microphone-accelerometer sensor pairs were used to record the mechanomyographic signals. A multisensor data fusion strategy for generation of binary control signals, based on the root-mean-square (RMS) values of the segmented signals, was trained and used as a detector (Silva et al. (2003)). Accuracies of 95% and 86% were achieved in the detection of contraction signals from the wrist extensors and flexors, respectively. Lopez et al. (2009) proposed two strategies for data fusion based on variance weighted average and decentralized Kalman filter, by means of an arrangement of redundant potentials, that is, by combining the SEMG signals. The muscle contraction amplitude was estimated and transformed to angular reference for the control of the robot joint. The algorithms demonstrated an efficient performance, and the joint never moved beyond its safety range (Lopez et al. (2009)).

Despite great success in decoding discrete movements such as individual finger flexion or extension, the matter of continuously predicting joint angles using SEMG signals is comparatively underdeveloped (Smith et al. (2008)). Increasing the number of SEMG channels that are acquired and processed may provide the user with higher accuracy in controlling the intensity of the contraction (Englehart et al. (2001)). However, as the number of inputs increases, the complexity of the network structure grows exponentially, which significantly increases the convergence time and the system response time. This chapter presents a feature extraction and pattern classification algorithm for estimating the intended knee joint angle from a two-channel SEMG signal, acquired using surface electrodes placed on the upper leg. This algorithm was designed for myoelectric control of an active transfemoral prosthesis (Cascão et al. (2005);Rodrigues et al. (2006)), as an improvement to the algorithm proposed by Ferreira et al. (2005). The proposed method improves the feature extraction stage by using a combination of spectral and temporal domain approaches – AR coefficients (Huang et al. (2005);Hargrove et al. (2008)) and signal amplitude histogram (Zardoshti-Kermani et al. (1995);Liu et al. (2007)), respectively – and by incorporating a feature projection stage, using a self-organizing map (SOM) (Kohonen (2001)). The incorporated Kohonen network reduces the dimensionality of the data at the input of the Levenberg–Marquardt (LM) neural classifier (Hagan & Menhaj (1994)), by mapping all the AR and histogram coefficients into a two-dimensional vector space (Chu et al. (2005)).

The accuracy of knee joint angle estimation algorithms based exclusively on pattern-recognition of SEMG signals may be greatly reduced by problems such as the required high level of amplification (due to the low level of the SEMG signals), motion of the sensor cables and/or noise caused by the power supplies (Merletti & Parker (2004)). These issues make myoelectric control rather sensitive. This motivates the use of other type of sensors on the prosthesis, which may potentially allow parameter adaptation during the use of the prosthesis by the patient. For example, micro-electromechanical gyroscopes and joint motion sensors may be used for measuring the angular velocity of the knee joint. The integration of these data can be used to obtain an estimate of the knee joint angle, which can be used to make small corrections of the neural network's coefficients in real-time. Fusion of the SEMG signals with proprioceptive sensor data could also improve the precision of the prosthesis control during movement and provide a more reliable myoelectric control (Oskoei & Hu (2007)).

This chapter presents various algorithms that use SEMG signals and proprioceptive sensors

for continuous estimation of the knee angle for control of active transfemoral prostheses. The next section presents the experimental protocol for SEMG signals and proprioceptive sensor data acquisition. Section 3 presents a knee angle estimation algorithm based exclusively on SEMG signal processing and analysis. Section 4 presents three algorithm variants based on data fusion of SEMG data and proprioceptive sensor (gyroscope) data. Section 5 proposes a performance comparison between the proposed algorithms. Results, discussions and conclusions are presented in sections 6, 7 and 8, respectively.

2. Experimental protocol and data acquisition

Myoelectric signal acquisition was performed using the microcontrolled bioinstrumentation system described by Delis et al. (2009b) and shown in Figure 2a. The system acquires two channels of amplified SEMG signals, the angular displacements signal and the data from the gyroscope sensors, using a 13-bit analog-to-digital converter, which is electrically isolated from the microcontroller and from the power supply using an optocoupler and a DC-DC converter. The sampling rate was 1043.45 Hz per channel. Analog filters are used to limit the SEMG signals to the 20–500 Hz frequency range (SENIAM (2008)). The microcontrolled system implements a digital real-time adaptive notch filter, which maintains a running estimate of the 60 Hz power line interference (Ahlstrom & Tompkins (1985)). The data is transferred to a personal computer through a serial interface. The experimental protocol was approved by the research ethics committee of the University of Brasilia (process no. 079/09, group III). Twelve able-bodied volunteers were studied and provided informed consent in accordance with institutional policy. Two pairs of 10-mm Ag/AgCl surface electrodes were placed in bipolar configuration over a pair of antagonist muscles (Figures 2b and 2c). These muscles correspond to the flexion and extension movements of the knee joint, respectively. The SEMG electrodes were attached to the skin over the muscle such that the longitudinal axes of the electrodes were parallel to the longitudinal axes of the muscle. The distance between the centers of the electrodes from each pair was 2–3 cm, according to the SENIAM protocol recommendations (SENIAM (2008)). The reference electrodes were placed over the lateralis and medialis epicondyle bones. An electrogoniometer was placed and strapped over the external side of the leg, and the gyroscope sensors were placed over the upper and lower legs, respectively (Figure 2d). The difference between the signals measured by the gyroscopes reflects the angular rate of the knee joint. Each of the twelve subjects was studied over the course of five days. Four 15-second measurements were performed on each day, with 5-minute rest periods between measurements. For each measurement, the subject was asked to walk in particular directions at a constant pace. Some variability in pace was observed between measurements. The first and third measurements from each day were used for training the algorithm's neural network, and the second and fourth measurements were used for testing the algorithm. Figure 3 presents simultaneously-acquired SEMG and proprioceptive signals from a representative subject. A total of 240 measurements were obtained, with half of them being used for algorithm training and the other half being used for algorithm testing.

3. Knee angle estimation based exclusively on SEMG data

The first proposed algorithm provides knee angle estimates based exclusively on information extracted from the electromyographic signals (Figure 4). The algorithm is composed of three main stages: (i) feature extraction, using a combination of spectral and temporal

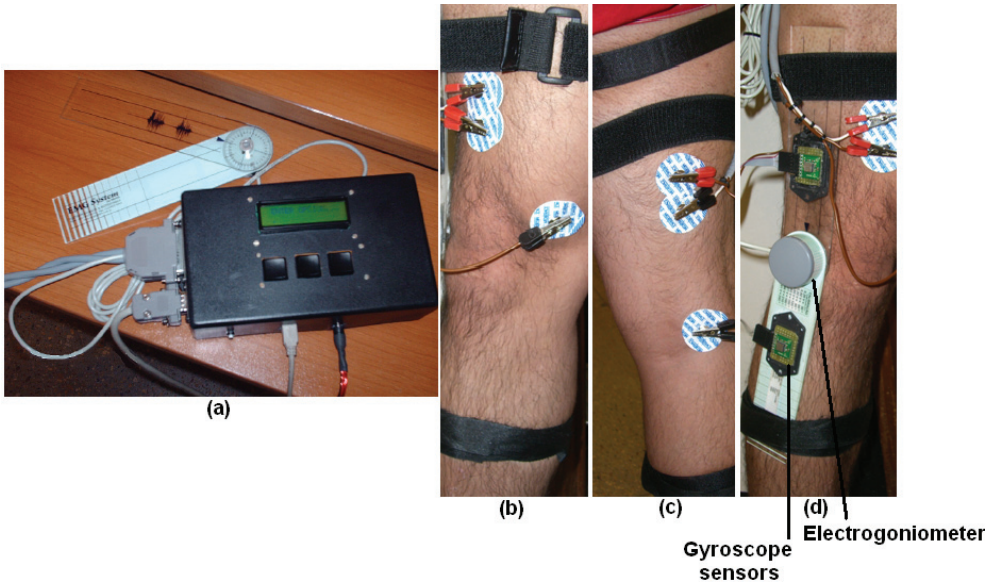

Fig. 2. Bioinstrumentation system (a) and placement of SEMG electrodes (b,c), electrogoniometer and gyroscope sensors (d).

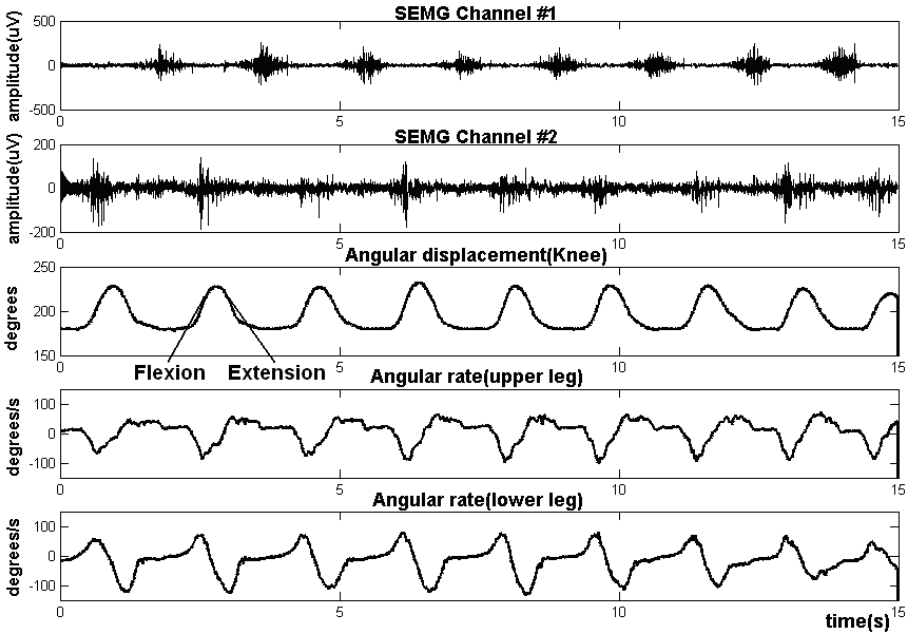

Fig. 3. Representative set of simultaneously-acquired SEMG signals, electrogoniometer angle and gyroscope measurements.

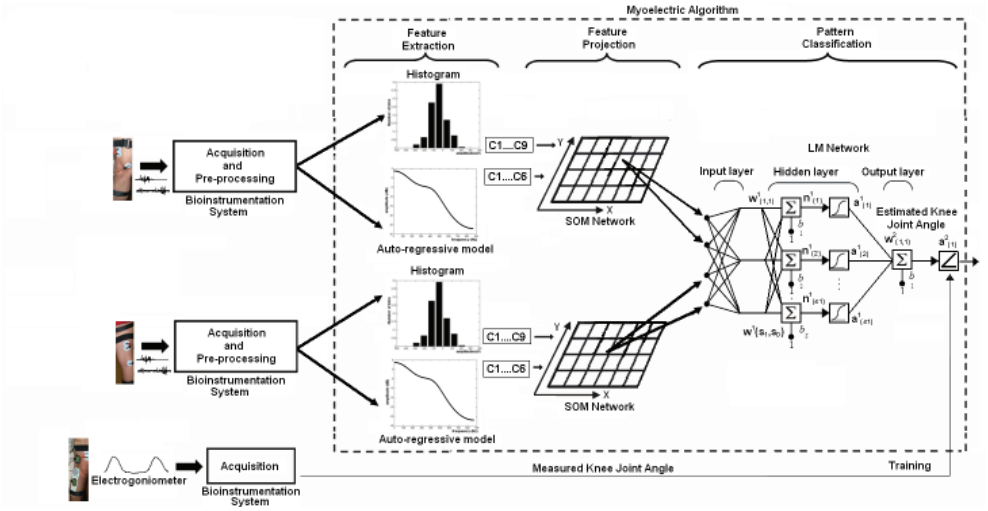

Fig. 4. Block diagram of the proposed knee joint angle estimation algorithm based exclusively on SEMG data.

domain approaches (AR coefficients and signal amplitude histogram, respectively); (ii) feature projection, using a self-organizing map; and (iii) pattern classification, using a Levenberg–Marquardt multi-layer perceptron neural network. Feature extraction and projection is performed independently for each SEMG channel. Data from the electrogoniometer is used as reference during network training, and is not used by the network during testing. Each of these stages is discussed in detail below, followed by a discussion on the approach for training the cascade networks.

3.1 Feature extraction

Presenting the myoelectric signal directly to a neural classifier is impractical, because of the dimensionality and random characteristics of the signal. The signal needs to be represented by a vector of reduced dimensionality, capable of representing the signal's information in a more compact fashion. Such vector is called a feature vector. In this work, the feature vector is composed of two sets of coefficients: the amplitude histogram bin counts, representing the time-domain characteristics of the SEMG signal, and the auto-regressive coefficients, representing the spectral content of the signal. The auto-regressive model is a convenient structure for model identification, in which the spectral envelope of the signal is modeled as an all-pole transfer function. The coefficients of this transfer function (the AR coefficients) contain information about the frequency content of the signal. In this work, the AR coefficients are used to compactly represent the spectral features of the SEMG signal (Huang et al. (2005); Hargrove et al. (2008)). The coefficients are calculated using the recursive least squares algorithm with a forgetting factor (Vaseghi (2000)). This gives more weight to the most recent samples at the moment of the iteration, which allows the algorithm to track temporal variations of the signal. The parameters are calculated recursively (Ljung (1987)) as presented

below:

$$\hat{\eta}_k = \hat{\eta}_{k-1} + L_k \left[y_k - \varphi_k^T \hat{\eta}_{k-1} \right], \quad (1)$$

$$P_k = \left[P_{k-1} - \frac{P_{k-1}\varphi_k \varphi_k^T P_{k-1}}{\lambda_k \varphi_k^T P_{k-1} \varphi_k} \right] \frac{1}{\lambda_k}, \quad (2)$$

$$L_k = \frac{P_{k-1}\varphi_k}{\lambda_k + \varphi_k^T P_{k-1} \varphi_k}, \quad (3)$$

where $\hat{\eta}_k$ are the vector coefficients that are estimated at discrete time k; φ_k is the regressors vector, P_{k-1} is the error covariance matrix and L_k is the gain vector of the filter. The forgetting factor λ_k controls the system response time. Based on literature (Huang et al. (2005);Ferreira et al. (2005)) and on an evaluation using the Akaike criterion (Ljung (1987)), we concluded that an AR order of four to six is sufficient for efficiently representing the SEMG signal. Thus, a sixth-order AR model was used, with a forgetting factor $\lambda_k = 0.995$, which is equivalent to 200 samples, or 192 ms. The coefficient estimated at instant k can be interpreted as a characteristic of the SEMG signal within the time interval specified by the forgetting factor, and it is a way of determining the angular displacement that the patient is trying to impose to the prosthesis (Ferreira et al. (2005)). The coefficients form a feature vector for the pattern classification process. This procedure is initialized with $P_0 = \mathbb{I}$ and $\hat{\eta}_0$ being a null vector.

The SEMG amplitude histogram is an extension of the zero crossing and the Willison amplitude measures (Zardoshti-Kermani et al. (1995)). The amplitude histogram provides a measure of the regularity in which the SEMG signal reaches each level of amplitude, associated with different histograms bins. Myoelectric signals reach relatively higher levels during the contraction period (compared to the base line amplitude), thus the amplitude histogram is capable of providing useful information about the state of a joint (Zardoshti-Kermani et al. (1995)). A histogram with nine symmetrically and uniformly distributed bins was used in this algorithm. The range of values was set based on the maximum and minimum SEMG amplitude levels measured on the training datasets. The window length was set to 200 samples (192 ms). Both the histogram window and the AR coefficients are updated for every new SEMG sample. This produces a more dense but semi-redundant stream of class decisions that could potentially be used to improve response time and accuracy (Englehart & Hudgins (2003)).

3.2 Feature projection

The feature extraction stage reduces the dimensionality of the data to fifteen (nine histogram bins, and six AR coefficients). The feature projection stage further reduces the dimensionality of the feature vector, by mapping it into a two-dimensional space using a self-organizing map. SOM neural networks (Kohonen (2001)) are trained using unsupervised learning, and are capable of arranging the input data into a discretized two-dimensional space (a map), which attempts to preserve the topological properties of the input space. The SOM is composed of nodes (or neurons). A position in the map space and a weight vector (of the same dimension as the input data vectors) are assigned to each node. The mapping algorithm consists in finding the node with the weight vector that is the closest to the input vector. The output of the SOM network is the two-dimensional coordinate of the winning node. To find the output neuron (winning node), the following steps are used, according to the learning rule of the Kohonen feature map (Haykin (1999)), applied to a SOM with N nodes trained with feature inputs x:

Step 1: Choose random values for the initial weight vectors $w_j(0)$.

Step 2: Find the winning neuron y_c at time step t (similarity matching), by using the minimum-distance Euclidean criterion:

$$y_c = \arg_{w_j(t)} \min \left\| x(t) - w_j(t) \right\|, j = 1,2,\ldots N \tag{4}$$

Step 3: Update the synaptic weight vectors of all neurons by using the following update rule:

$$w_j(t+1) = w_j(t) + \rho(t) h_{j,y_c}(t) \left[x(t) - w_j(t) \right] \tag{5}$$

where $\rho(t)$ is the learning rate, and $h_{j,y_c}(t)$ is the neighbor function centered around the winner y_c. $\rho(t)$ and $h_{j,y_c}(t)$ are changed dynamically during the learning stage, in order to obtain optimal results.

Step 4: Go back to Step 2 until no changes in the feature map are observed.

Each of the two SOM maps (one for each SEMG channel) is arranged in a topological net with 100 neurons in their interconnection structure (10×10 matrix). The dimension of the network was chosen empirically, based on experimentation. The initial learning rate was 0.9, and the time constants τ_1 and τ_2 were 1431 and 1000 iterations, respectively (Haykin (1999)). The neighborhood function initially contains all the neurons of the network, centered around the winning neuron, and with time it gradually decreases in size. Thus, the initial size of the neighborhood function is equal to the radius of the lattice (i.e., 5). At the output of the feature projection stage, the information in each of the SEMG channels is represented by only two coefficients, i.e., a 2D coordinate, resulting in a total of four coefficients at the input of the pattern classification stage. Different coordinate pairs represent different points of operation associated with the movement of the knee joint during a walk.

3.3 Pattern classification

The pattern classification stage is responsible for providing an estimate of the knee joint angle from the set of four SOM coefficients obtained from the feature projection stage. This is performed using a Levenberg–Marquardt multi-layer perceptron neural network (Hagan & Menhaj (1994)). There has been considerable research on methods to accelerate the convergence time of multi-layer feed-forward neural networks, such as methods that focus on standard numerical optimization techniques, including the conjugate gradient algorithm, quasi-Newton methods, and nonlinear least squares (Battiti (1992); Charalambous (1992)). The method used in this chapter is an application of a nonlinear least squares algorithm to the batch training of multi-layer perceptrons, called Levenberg–Marquardt algorithm. The LM algorithm is very efficient for training moderate-sized feed-forward neural networks (Hagan & Menhaj (1994)). Although the computational requirements of the LM algorithm become much higher after each iteration, this is fully compensated by its higher efficiency. This is especially true when high precision is required. Similarly to the quasi-Newton methods, the LM method was designed to approach second-order training speed without computing the Hessian matrix. The key step in the LM algorithm is the computation of the Jacobian matrix, which can be computed through standard backpropagation techniques (Hagan & Menhaj (1994)), which are much less complex than computing the Hessian matrix.

The LM network used in our algorithm has three layers in its structure, with four input nodes (output vectors of the SOM networks) in the first layer, six nodes in the second layer (associated with tangential functions), and one node in the output layer (associated with a linear function). This structure was chosen empirically, based on experiments aimed at

minimizing the mean squared error (MSE). The node in the output layer represents the estimated knee joint angle (Figure 4).
The cascade networks (SOM and LM) were trained independently for each set of 15-second two-channel SEMG test signals, using its correspondent set of training signals and electrogoniometer measurements. First, the histogram and AR coefficients associated with each sample of each of the two SEMG signals were calculated. Then, these coefficients were used in the SOM networks' unsupervised training process to configure the topological map structures and set the weight vector of each neuron. Then, the same feature vectors were used into the trained SOM maps, in order to generate two-dimensional vectors to be used for training the LM network. During LM network training, the outputs from the trained SOM network were used as inputs, and the corresponding angular displacement measurements from the electrogoniometer were used as the target outputs. The same initial weight values were used for all three network layers (zero for all neurons). The maximum number of iterations was set to 50, the MSE stop criterion was 10^{-10} n.u.^{2}, and the initial learning rate was 1.0. These values were empirically chosen, aiming at maximum reduction of the final MSE.

4. Knee angle estimation based on fusion of SEMG and proprioceptive sensor data

Angular rate information may be extracted from gyroscope sensor data using a Kalman filter. This approach was evaluated in three myoelectric algorithm variants. The angular rate information is used to correct the estimation of the intended knee joint angle by fusion with the SEMG features. The three algorithms are composed of a feature extraction stage, a pattern classification stage and variations of a data fusion stage.

4.1 Feature extraction

For this data fusion approach, the set of features is obtained from Cepstral coefficients extracted from SEMG signals. Cepstral analysis is used for frequency-domain SEMG signature discrimination. The cepstrum of a signal is defined as the inverse Fourier transform of the logarithm of the squared magnitude of the Fourier transform of a signal (Kang et al. (1995)). If all transfer function poles are inside the unit circle, the logarithmic transfer function can be represented as a Laurent expansion (Kang et al. (1995)). Hence, the following recursive relation may be used to calculate cepstral coefficients from AR coefficients:

$$\begin{aligned} c_1 &= -a_1 \\ c_i &= -a_i - \sum_{n=1}^{i-1} \left(1 - \frac{n}{i}\right) a_n c_{i-n}, \quad i = 2, ..., P. \end{aligned} \tag{6}$$

Using (6), the first P cepstral coefficients (c_i, $i = 1, ..., P$) can be obtained from the coefficients (a_k) of a Pth order AR model, estimated as in Section 3.1. Some works have reported that the AR-derived cepstrum feature has better performance than the unprocessed AR feature (Kang et al. (1995) ; Chiou et al. (2004)). Even though the cepstral coefficients are derived directly from the AR coefficients, they do not contain exactly the same information, because the recursive operation changes the distribution of the features nonlinearly (Kang et al. (1995)). In this work, the cepstral coefficients were obtained using a sixth-order AR model and (6).
A second approach for feature extraction is implemented using the entropy of the myoelectric signal, calculated and used as a time-domain feature vector (Ito et al. (2008)). We focus on the difference in entropy between the stationary SEMG signal in a relaxed state and

during motion. Assuming that electromyographic signals can be approximated by a normal distribution process with zero mean, the entropy of the distribution in a M-sample time window is computed as

$$H(\sigma_i) = \frac{1}{2}\log(2\pi\sigma_i^2), \tag{7}$$

$$\sigma_i^2 = \frac{1}{M-1}\sum_{m=0}^{M-1} x_i^2(k-m), \tag{8}$$

where σ_i^2 represents the signal variance estimated from the signal measured from each electrode and x_i is the SEMG signal from the i-th electrode (Ito et al. (2008)). For each SEMG channel, the calculated entropy is concatenated with the cepstral feature vector. This combination provides robustness in weak SEMG signals.

4.2 Pattern classification

The pattern classification stage is implemented using a LM neural network, just as described in Section 3.3.

4.3 Data fusion strategies

Three data fusion strategies for estimating the intended knee joint angle were evaluated: (i) data fusion implemented during pattern classification, which is performed on both SEMG features and estimated angular rate; or (ii, iii) data fusion performed after pattern classification, which is performed on the SEMG features only. These strategies are presented next.

4.3.1 First data fusion strategy

Figure 5 presents the block diagram for the proposed knee angle estimation algorithm based on the first data fusion strategy. The use of angular rate information from the gyroscopes improves angle estimation precision and reduces estimation artifacts. Feature extraction is performed using a Kalman filter. The goal of Kalman filters is the estimation of non stationary noisy signals, by minimizing the mean squared error, i.e., recursive least squares for stochastic models. The estimated signal is modeled using a state-space formulation, describing its dynamical behavior (Diniz (1997)), according to the following first-order linear stochastic model:

$$x(k) = x(k-1) + n(k) \tag{9}$$

$$y(k) = x(k) + v(k) \tag{10}$$

where $x(k)$ is the joint angular rate, $n(k)$ is the noise modeling the evolution of the joint angular velocity between two sampling intervals, $y(k)$ is the measured angular rate, obtained from subtracting the angular rate values measured on the upper and lower legs, respectively; and $v(k)$ is the measurement noise. It is assumed that $n(k)$ and $v(k)$ are zero mean, uncorrelated Gaussian distributions, with variances q^2 and r^2, respectively. When applying the Kalman filter to this model, the prediction process for each iteration cycle is expressed according to

$$\hat{x}(k|k-1) = \hat{x}(k-1) \tag{11}$$

$$P(k|k-1) = P(k-1) + q^2 \tag{12}$$

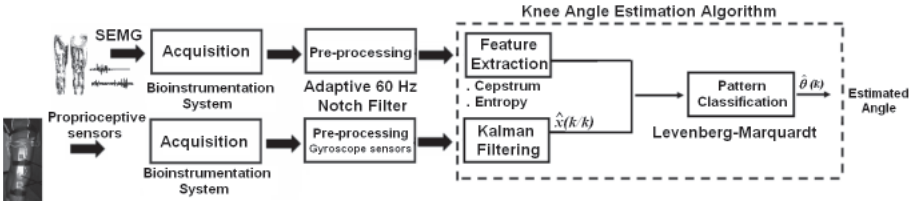

Fig. 5. Block diagram of the proposed knee angle estimation algorithm based on the first fusion strategy.

where $P(k|k-1)$ is the predicted error covariance matrix. The algorithm is initialized as $q^2 = 4$, $r^2 = 10$, $\hat{x}(0) = 0$ and $P(0) = 0.01$. These predictions are corrected, using the angular rate measure provided by the gyroscopes, $y(k)$, as follows:

$$G(k) = \frac{P(k|k-1)}{P(k|k-1) + r^2} \tag{13}$$

$$\hat{x}(k) = \hat{x}(k|k-1) + G(k)\left(y(k) - \hat{x}(k|k-1)\right) \tag{14}$$

$$P(k) = \left(\mathbb{I} - G(k)\right) P(k|k-1) \tag{15}$$

where $G(k)$ is the Kalman filter gain, and $\hat{x}(k)$ is an optimal estimate of $x(k)$ in the least-squares sense. It can be shown that, for this specific problem, this filter is equivalent to a unity-gain, low-pass, first-order filter with time-varying cut-off frequency. This cut-off frequency is computed considering noise variances q^2 and r^2, as well as the error variance associated with $\hat{x}(k)$ (Diniz (1997)). The value of $\hat{x}(k)$ is an optimal estimate of the mean of the knee joint angular rate at sampling step k. Thus, at each time instant k, the optimally filtered angular rate estimate $\hat{x}(k)$, along with the SEMG cepstral and entropy coefficients are used as inputs to the neural classifier (Figure 5).

4.3.2 Second data fusion strategy

The second data fusion strategy is based on information fusion in the correction process of a Kalman filter. This may reduce the perturbations that are generated on the angle estimation process from the neural network. This data fusion strategy is presented in Figure 6. In this strategy, the feature vectors obtained from feature extraction are used as inputs to the LM neural network. The estimated knee joint angle is modeled using a state-space formulation, describing its dynamical behavior (Diniz (1997)), according to the following linear stochastic model:

$$x(k) = x(k-1) + Tu(k) + n(k) \tag{16}$$

$$y(k) = x(k) + v(k) \tag{17}$$

where $x(k)$ now represents the knee angle, $u(k)$ is the measured angular rate acquired with a sampling period T, obtained from subtracting the angular rate values measured on the upper and lower legs, respectively. $n(k)$ is noise modeling the evolution of the knee joint angle between two sampling intervals. $y(k)$ is the measured knee joint angle obtained from the LM neural network output, and $v(k)$ is the associated measurement noise. It is assumed that $n(k)$ and $v(k)$ are zero mean, uncorrelated Gaussian distributions, with variances q^2 and r^2, respectively. When applying the Kalman filter to this model, the prediction process for each

iteration cycle is expressed according to

$$\hat{x}(k|k-1) = \hat{x}(k-1) + Tu(k) \quad (18)$$

$$P(k|k-1) = P(k-1) + T^2\sigma_u^2(k) + q^2 \quad (19)$$

where $\sigma_u^2(k) = 25\ \text{deg}^2\ /\ \text{sec}^2$ is the variance of the measured angular rate information $u(k)$. q^2, r^2, $\hat{x}(0)$ and $P(0)$ have the same values as in the previous strategy, and the correction process is expressed by the same equations, (13)-(15). However, the value $\hat{x}(k)$ is an optimal estimate of the knee joint angle from the fusion process at each time instant k.

4.3.3 Third data fusion strategy

A third variant is a modification of the previous strategy. This variant introduces a compatibility test based on the Mahalanobis distance (De Maesschalck et al. (2000)). The Mahalanobis distance is a useful way of determining similarity of sample sets, as it is not dependent on the scale of the measurements. The Mahalanobis distance is computed between the prediction and correction process of the Kalman filter (Figure 7). The objective is to detect possible artifacts that come from the estimated angle at the LM neural network output, on each time step of the data fusion process.

When the Kalman filter is applied to the linear stochastic model described by equations (16) and (17), the prediction process for each iteration cycle is described by equations (18) and (19). The Mahalanobis distance is calculated between the estimated knee angle $y(k)$ from the LM neural network and the predicted knee angle $\hat{x}(k|k-1)$, based on the following equations:

$$d^2(k) = \frac{(y(k) - \hat{x}(k|k-1))^2}{P(k|k-1) + r^2}. \quad (20)$$

It can be shown that $d^2(k)$ is χ_1^2 distributed. Thus, $y(k)$ and $\hat{x}(k|k-1)$ are said to be statistically compatible if $d^2(k) \leq 3.81$, according to the 95% confidence threshold obtained from the chi-square table. In such a case, $y(k)$ is used to correct $\hat{x}(k|k-1)$ using equations (13)-(15). If $d^2(k) > 3.81$, the filter uses the predicted values as estimates: $\hat{x}(k) = \hat{x}(k|k-1)$ and $P(k) = P(k|k-1)$, protecting the estimation process from possible angle estimation artifacts at the neural network, originated from SEMG signals.

4.4 Parameter setting for the myoelectric algorithms based on data fusion

Network training and testing were performed in Matlab (The MathWorks, Inc., Natick, MA, USA). For each SEMG channel, the proposed algorithms were implemented using 200 sample (192 ms) sliding windows for the feature extraction process (cepstral analysis and entropy).

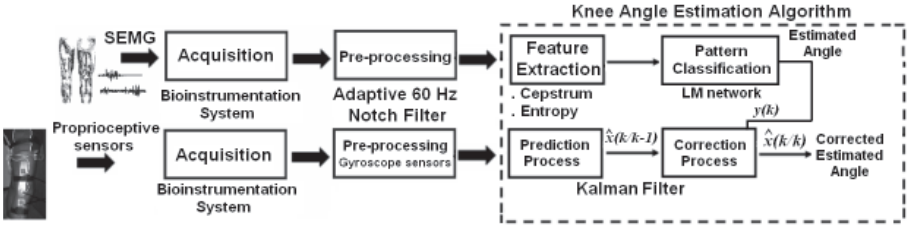

Fig. 6. Block diagram of the proposed knee angle estimation algorithm based on the second fusion strategy.

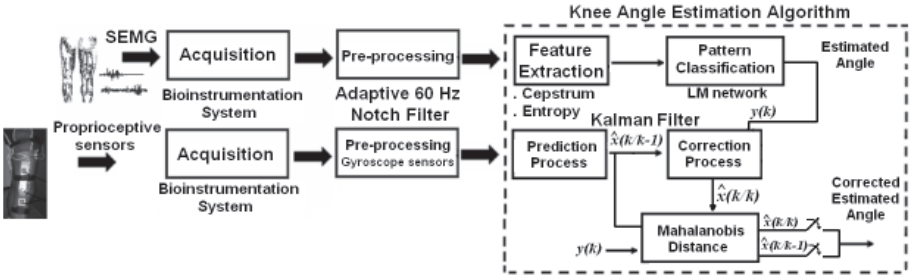

Fig. 7. Block diagram of the proposed knee angle estimation algorithm based on the third fusion strategy.

For each new pair of gyroscope sensor samples, estimates of updated Kalman filter angular rate (first proposal) and knee joint angle (second and third proposals) were calculated. This results in a 15-coefficient feature vector per sample interval (six cepstral coefficients and one entropy coefficient per SEMG channel, plus one angular rate coefficient) for the first proposal. For the second and third proposals, we obtained a 14-coefficient feature vector (6 cepstral coefficients and 1 entropy coefficient, per SEMG channel). In the three algorithms, the information is transferred to a LM neural network, with 15 (first proposal) or 14 (second and third proposals) nodes in the input layer, 6 nodes in the hidden layer, and 1 node in the output layer. The output node represents the estimated knee joint angle. The network architecture and size was empirically chosen, aiming at maximum reduction of the final MSE. The same initial weight values were used for all three network layers (zero for all neurons). The maximum number of iterations was set to 50, the MSE stop criterion was 10^{-10} n.u^2. and the initial learning rate was 1.0. The true displacement angle measured with the electrogoniometer was used as training reference.

5. Performance comparison between the proposed algorithms

For performance evaluation, the myoelectric algorithms are quantitatively compared using statistics metrics based on: (i) the error-to-signal percentage, (ii) the correlation coefficient and (iii) statistics of error events, including the number of error events, the maximum error event duration and the maximum error amplitude (Delis et al. (2009a)). The statistics were calculated for each set of SEMG signals, and the average and standard deviation of those parameters were calculated for each subject. For consistency, the same training process and test sets were used with the myoelectric algorithms based solely on SEMG signals and with those based on data fusion. The same sliding window length (192 ms) and step (1 sample) and the same AR order and forgetting factor configuration were used for all evaluated methods. 120 sets of SEMG, electrogoniometer and gyroscope data which were not used for training were used for comparing the methods. The performance of each algorithm was evaluated by comparing the knee angle estimated from the SEMG signals with the angular displacement values measured with the electrogoniometer.

A threshold was applied to the time-series to detect the error events (Delis et al. (2009a)). This threshold was empirically set to 10°. Each series of consecutive errors found to be above the threshold was considered an error event.

The Mahalanobis distance was calculated for each metric as a means of assessing the statistical difference between the proposed method based solely on the SEMG signals and the proposed

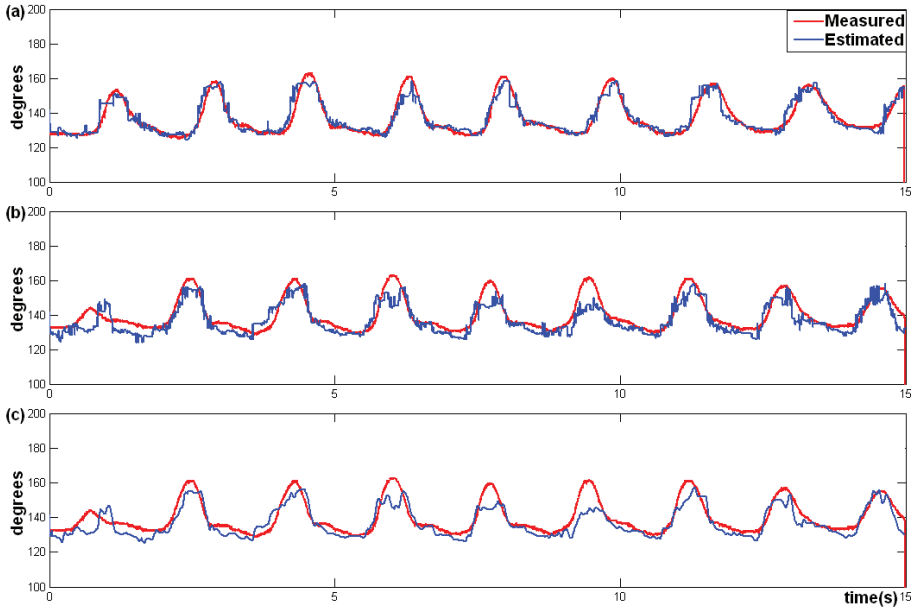

Fig. 8. Knee angle estimation results for the algorithm based exclusively on SEMG data, (compared with the electrogoniometer measurements) for two sets of signals from the same subject: (a) training results; (b) test results; (c) filtered test results.

methods based on data fusion (Delis et al. (2009a);Duda & Hart (2000)). For $N = 12$ datasets, the Mahalanobis distance between a same metric computed using two techniques, represented by m_1 and m_2, is given by

$$d^2_{m_1 m_2} = \sum_{n=1}^{N} \frac{(m_1(n) - m_2(n))^2}{\sigma_1^2 + \sigma_2^2} \tag{21}$$

$$\sigma_i^2 = \frac{1}{N-1} \sum_{n=1}^{N} \left(m_1(n) - \frac{1}{N} \sum_{n=1}^{N} m_i(n) \right)^2, \quad i = 1,2$$

where n means the n-th dataset. The metrics m_1 and m_2 are considered to be statistically similar (with 95% confidence) if $d^2_{m_1 m_2} \leq 21.03$, which is equivalent to $d_{m_1 m_2} \leq 4.58$.

6. Results

6.1 Testing process

Figure 8 presents two time-series of estimated knee joint angle from a subject, obtained during the training and testing processes, respectively, using the algorithm based exclusively on SEMG data. In the test results, a 50-tap (48 ms) moving average filter was used for reducing the estimation noise and the variance (Figure 8c). Such filtering removes jitter in the output signal, which could cause undesirable and unintentional motion of the prosthesis. The results were satisfactory, with a reduction of impulsive noise and maintaining the slope change in the estimated angle.

Figure 9 shows three time series for estimated knee angle by the proposed myoelectric algorithms based on data fusion. It can be noted that the three algorithm variants provide good tracking of the knee angle with respect to the measured angle, in spite of the occurrence of discrete artifacts. Such artifacts may be imperceptible for myoelectric control, because of the prosthesis' mechanical inertia.

6.2 Comparison between the proposed algorithms

Figure 10 presents a qualitative comparison between the myoelectric algorithms based exclusively on SEMG data and those based on data fusion. Measured and estimated angle displacements from a subject are shown for (a) the first proposal based solely on SEMG signals; (b) the first variant based on data fusion; (c) the second variant based on data fusion; and (d) the third variant based on data fusion. The absolute difference between measured and estimated angles is also shown.

Figure 11 presents a similar qualitative comparison, but in the presence of motion artifacts. The straps holding the electrode cables were intentionally left loose during this experiment, which caused motion artifacts in the SEMG signal. Measured and estimated angle displacements from a subject are shown for (a) the algorithm based exclusively on SEMG signals; (b) the first variant based on data fusion; (c) the second variant based on data fusion; and (d) the third variant based on data fusion. The absolute difference between measured and estimated angles is also shown. In spite of the occurrence of false positives during the knee joint angle estimation process with the proposed algorithms, the level of degradation of the estimate is lower with the algorithms based on data fusion. The second and third variant presents errors peaks that could be imperceptible for the movement of the leg prosthesis,

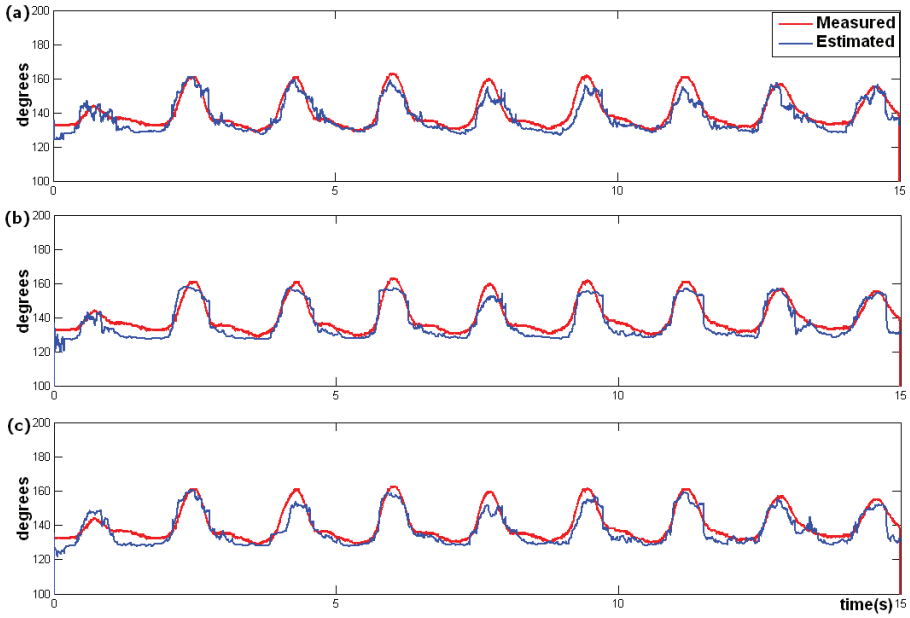

Fig. 9. Measured and estimated knee joint angle for the three proposed algorithms based on data fusion: (a) first variant; (b) second variant; (c) third variant.

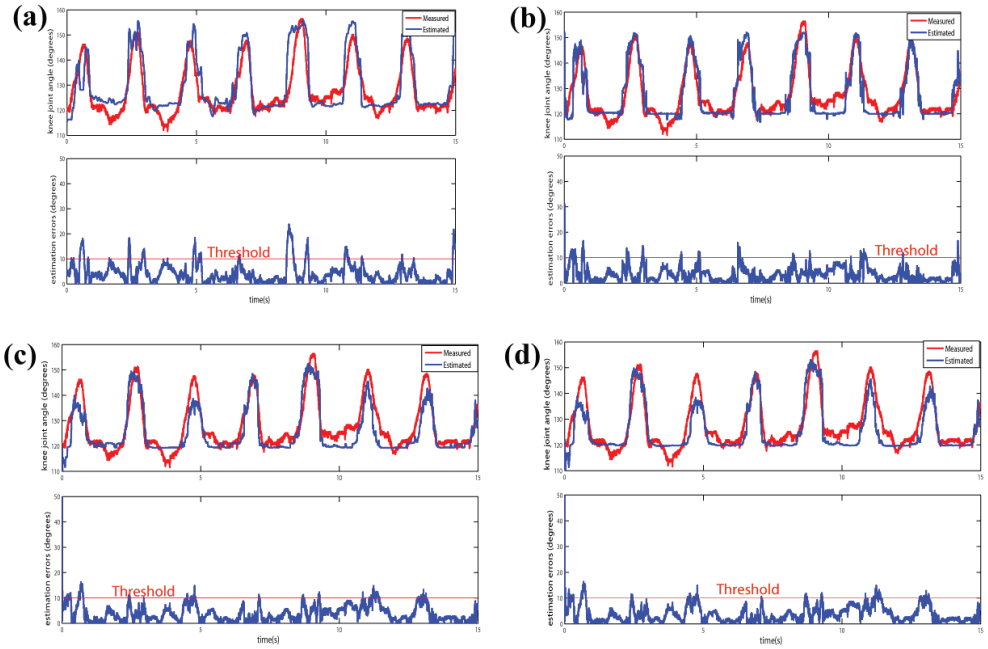

Fig. 10. Qualitative comparison between the proposed myoelectric algorithms. Measured and estimated displacement angle from a representative experiment and their absolute differences (estimation error) are shown for the following algorithms: (a) first proposal based solely on SEMG signals; (b) first variant based on data fusion; (c) second variant based on data fusion; and (d) third variant based on data fusion.

depending on their duration. The best results in the presence of motion artifacts were obtained with the second and third data fusion variants, in which the fusion process is implemented between the SEMG signals and the gyroscopes sensors on the correction process by Kalman filtering.

Another implemented test was the evaluation of the robustness against power line 60-Hz interference. A 60-Hz signal with an amplitude of 0.1 mV was added to each SEMG channel. This amplitude value was chosen for this test because this was the maximum 60-Hz interference level registered during the experiments. Figure 12 presents a qualitative comparison between the estimated and measured angles. Measured and estimated angle displacements from a subject are shown for (a) the first algorithm based exclusively on SEMG signals; (b) the first variant based on data fusion; (c) the second variant based on data fusion and (d) the third variant based on data fusion. The absolute difference between measured and estimated angles is also shown. It is observed that, in spite of the presence of discrete false positives, the estimated knee joint angle for the myoelectric algorithms is reasonably similar to the measured angle.

Table 1 presents the computed Mahalanobis distance – see equation (21) – between each method based on data fusion and the algorithm proposal based solely on SEMG signals. According to the threshold $d_{m_1 m_2} \leq 4.58$, only the first data fusion variant strategy presented statistically different results for the maximum error event amplitude metric. That means

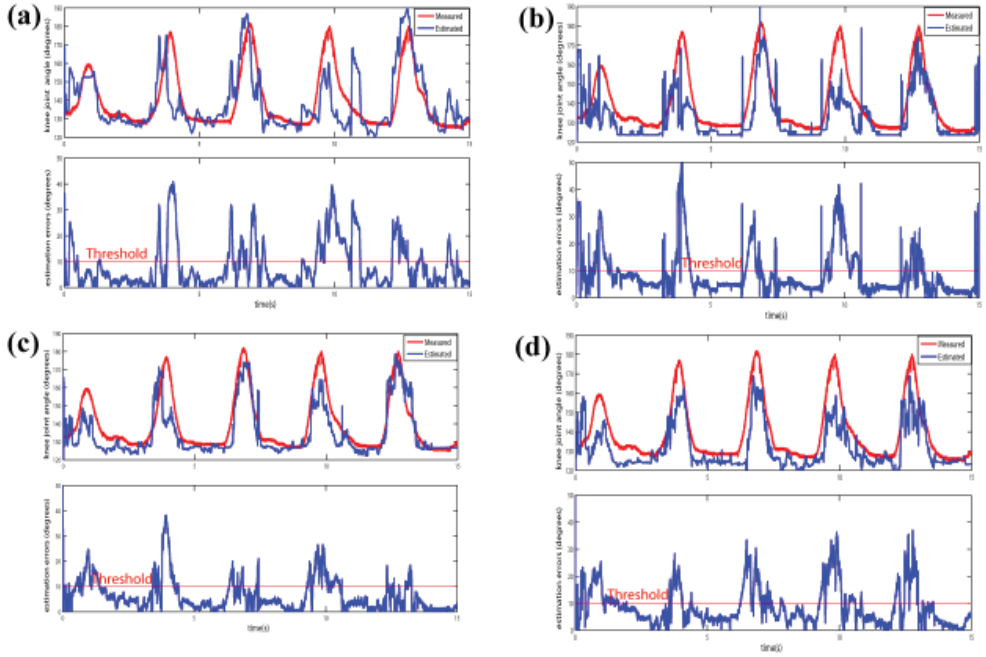

Fig. 11. Qualitative comparison between the proposed myoelectric algorithms. Measured and estimated angle displacements from measurements with movement artifacts and their absolute difference (estimation error), are shown for the following algorithms: (a) first proposal based exclusively on SEMG signals; (b) first variant based on data fusion; (c) second variant based on data fusion; (d) third variant based on data fusion.

that the second and third data fusion strategies present results which are similar in mean. However, the robustness of the third strategy with respect to SEMG artifacts is superior, as seen in the previous figures.

7. Discussion

The proposed myoelectric algorithms provide dimensionality reduction that makes possible the connection of a larger number of SEMG sensors without affecting the performance of the Levenberg–Marquardt multi-layer perceptron neural network. The algorithms based

Metric	First strategy	Second strategy	Third strategy
Error-to-signal percentage	1.61	1.00	1.53
Correlation coefficient	1.59	1.37	1.37
Number of error events	2.67	1.33	1.21
Maximum error event amplitude	17.30	1.27	1.07
Maximum error event duration	0.90	0.87	0.85

Table 1. Mahalanobis distance $d_{m_1 m_2}$ between each of the algorithm variants based on data fusion and the myoelectric algorithm based exclusively on SEMG signals.

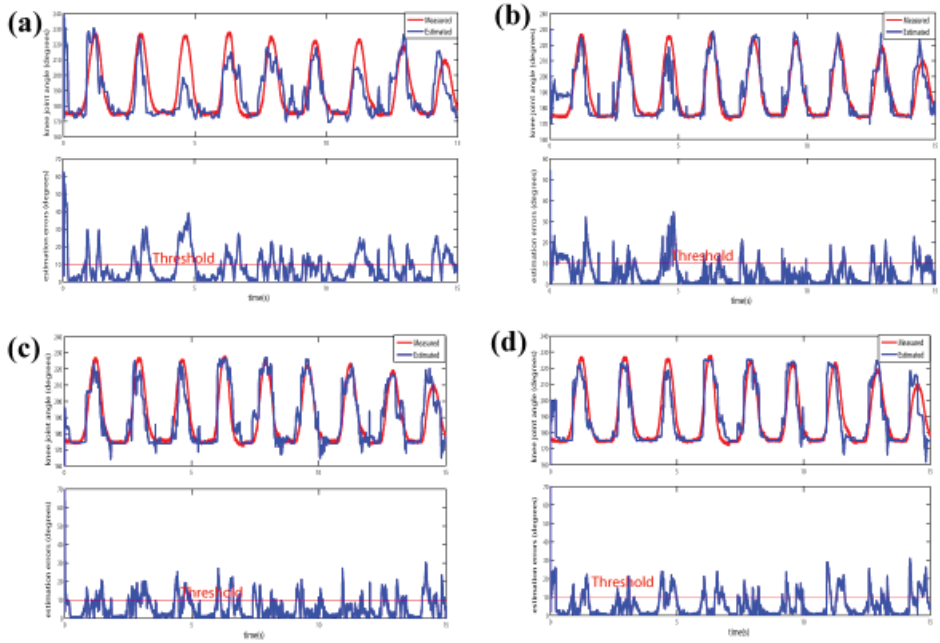

Fig. 12. Qualitative comparison between the proposed myoelectric algorithms. Measured and estimated angle displacements from measurements with added 60 Hz interference and their absolute difference (estimation error) are shown for the following algorithms: (a) algorithm based solely on SEMG signals; (b) first variant based on data fusion; (c) second variant based on data fusion; (d) third variant based on data fusion.

on data fusion makes possible the integration of different types of sensors, besides SEMG signals, using a Kalman filter. The access to additional information by the myoelectric algorithms during knee angle estimation improves precision and robustness for the prosthesis myoelectric control.

The maximum error amplitudes measured with the proposed methods are considerably reduced; however, they are still large (Figure 10, 11 and 12). Nevertheless, this may not be a significant issue, as short duration error events are unnoticeable to the leg prosthesis, due to the system's mechanical inertia. These short duration error peaks may be caused due to noise in the feature space, and/or by an insufficient number of neurons in the SOM network and in the LM network's hidden layer. This problem may be addressed by increasing the number of neurons, by increasing the number of SEMG signals, and/or adding other variables associated with leg proprioception (e.g., accelerometers). These approaches would result in increased computational network complexity and convergence time. Alternatively, error peaks may be avoided by increasing the forgetting factor of the recursive least squares AR algorithm and the window length of the histogram. However, this approach would increase the response time of the prosthesis. The accuracy of the proposed method in the presence of transient data may be improved using time-frequency and time-scale feature projection (e.g., wavelets, short-time Fourier transform) (Englehart et al. (2001)). However these approaches are more computationally intense than the combination of AR coefficients

with an amplitude histogram, as proposed in this work, and would also affect the networks' complexity. Furthermore, time-domain and AR features have been shown to outperform time-frequency features for stationary or slowly changing data, and to provide equivalent results for steady-state SEMG signals (Huang et al. (2005)).

The comparison of the first variant of the algorithm based on data fusion with the algorithm based exclusively on SEMG data showed a significant reduction on the maximum amplitude of error event. This emphasizes the fusion in the LM neural network of the information from the feature extraction process (cepstral coefficients and SEMG entropy) with the low-pass filtered angular rate information obtained from the Kalman filter. This fusion removes the noise on the estimated knee joint angle. It is expected that an increase in the amount of information supplied to the myoelectric algorithms (e.g., number of input channels) in the estimate process of the knee joint angle may result in improved precision for the control of the leg prosthesis.

The presence of artifacts due to movement of the electrode cables and 60-Hz interference during knee angle estimation may be interpreted by the leg prosthesis as false positives, depending of their duration (Figure 11b). The second and third variants based on data fusion, which use an optimal estimate of the knee joint angle obtained on the fusion process with the angular rate information at each time instant, are more robust than the myoelectric algorithms based solely on SEMG signals (Figures 11 and 12). The addition of other variables associated with leg proprioception (e.g., gyroscope sensors) may improve the precision and reduce artifacts in knee angle estimation, without significantly increasing the computational complexity of the myoelectric algorithm. However, the implementation of these algorithms involves an additional degree of complexity for obtaining the cepstral coefficients from the AR coefficients, in comparison with the first myoelectric algorithm proposal.

The first proposal is preferred for on-line implementation when the number of sensors is large and computational power is limited. However, considering the robustness aspect in the presence of movement artifacts, the second proposal based on data fusion is recommended.

Although the computational complexity of the Levenberg–Marquardt algorithm increases after each iteration during the training process, this is compensated by a gain in efficiency and a reduction in the network's convergence time. Hagan & Menhaj (1994) present comparisons between the Levenberg–Marquardt algorithm and modifications implemented in the back-propagation neural network, based in the conjugate gradient and variable learning rate. The results show failure in the convergence time for the evaluated modifications, while the same tests converged with acceptable results with the Levenberg–Marquardt algorithm. The results indicate that the LM algorithm is very efficient when it is trained with hundreds of neurons in their interconnection structure.

8. Conclusions

This chapter introduced a myoelectric algorithm based solely on SEMG data and three variants of myoelectric algorithms based on data fusion with the purpose of improving the knee joint angle estimation. The first proposal improves the algorithm originally presented by Ferreira et al. (2005), by adding a feature projection stage (a SOM network), and by incrementing the feature extraction stage with a signal amplitude histogram. Feature extraction now combines time-domain (histogram) and frequency-domain (AR coefficients) features. Pattern classification is still performed using a Levenberg–Marquardt multi-layer perceptron neural network, but this is now more efficient due to the dimensionality reduction provided by the SOM network.

The second proposal was based on three algorithm variants, which implement data fusion using Kalman filters. Through a prediction-correction formulation process, this provides an optimal estimate of the estimated knee angle, which is obtained by fusion of the information from gyroscope sensors using a Kalman filter. The myoelectric algorithms strategies present a feature extraction process based on cepstral coefficients and the entropy of the myoelectric signals (mixture of coefficients in frequency and time domains, respectively). A Levenberg–Marquardt multi-layer perceptron neural network is used for pattern classification. It was demonstrated that the fusion of SEMG signals with proprioceptive sensors reduces artifacts in the estimated joint angles.

The three algorithm variants based on data fusion present equivalent results when compared with the myoelectric algorithm based exclusively on SEMG signals, however, their performance is better in the presence of signal artifacts.

The concepts used in these algorithms may be useful in the development of a control algorithm for active leg prostheses, in which signals from many different sensors may be fused and used in the conception of a movement predictive model. We have demonstrated that it is possible to continuously decode knee position from SEMG signals collected from a generalized electrode placement in an able-bodied subject.

9. Acknowledgment

This work was partially supported by Brazilian Ministry of Education (MEC/CAPES), Brazilian Ministry for Science and Technology (MCT/CNPq), and Research and Graduate Council of the University of Brasilia.

10. References

Ahlstrom, M. L. & Tompkins, W. J. (1985). Digital filters for real-time ECG signal processing using microprocessor, IEEE Trans. Biomed. Eng., Vol. 32, pp. 708-713.

Battiti, R. (1992). First and second order methods for learning: between steepest decent and Newton's method, Neural Comput., Vol. 4, pp. 141-66.

Cascão, Jr. C. A.; Ferreira, R. U.; Beckmann, E. D.; Borges, G. A.; Ishihara, J. Y. & da Rocha, A. F. (2005). Estudo e desenvolvimento de uma prótese ativa de perna comandada por sinais eletromiográficos, Proceedings VII Simpósio Brasileiro de Automação Inteligente / II IEEE Latin-American Robotics Symp.

Charalambous, C. (1992). Conjugate gradient algorithm for efficient training of artificial neural networks, IEE Proc. G, Vol. 139, pp. 301-10.

Chiou, Y.; Luh, J.; Chen, S.; Lai, J. & Kuo, T. (2004). The comparison of electromyographic pattern classifications with active and passive electrodes, Medical Engineering and Physics, Vol. 26, No. 7, pp. 605-610.

Chu, J. U.; Moon, I.; Kim, S. K. & Mun, M. S. (2005). Control of multifunction myoelectric hand using a real time EMG pattern recognition, Proceedings IEEE/RSJ Int. Conf. Intelligent Robots and Systems, pp. 3957-62.

Dasarathy, B. V. (1997). Sensor fusion potential exploitation-innovative architectures and illustrative applications, Proceedings IEEE, pp. 24-38.

De Maesschalck, R.; Jouan-Rimbaud, D. & Massart, D. L. (2000). The Mahalanobis distance, Chemometrics and Intelligent Laboratory Systems, Vol. 50, pp. 1-18.

De Luca, C. J. (2006). Electromyography. Encyclopedia of Medical Devices and Instruments, John Wiley Publisher, pp. 98-109.

Delis, A. L.; Carvalho, J. L. A.; da Rocha, A. F.; Ferreira, R. U.; Rodrigues, S. S. & Borges, G. A. (2009a). Estimation of the knee joint angle from surface electromyographic signals for active control of leg prostheses, Physiological Measurements,Vol. 30, pp. 931-946.

Delis, A. L.; Carvalho, J. L. A.; da Rocha, A. F.; Nascimento, F. A. O. & Borges, G. A. (2009b), Development of a Myoelectric Controller Based on Knee Angle Estimation, Proceedings International Conference on Biomedical Electronics Devices, pp. 97-103.

Diniz, P. S. R. (1997). Adaptive Filtering Algorithms and Practical Implementation, Kluwer Academic Publishers.

Duda, R. O.; Hart, P. E. and Stork, D. G. (2000). Pattern Classification, John Wiley, 2nd edn, New York.

Englehart, K.; Hudgins, B. & Parker, P. A. (2001). A wavelet-based continuous classification scheme for multifunction myoelectric control, IEEE Trans. Biomed. Eng., Vol. 48, pp. 302-10.

Englehart, K. & Hudgins, B. (2003). A robust, real time control scheme for multifunction myoelectric control, IEEE Trans. Biomed. Eng., Vol. 50, pp. 848-54.

Ferreira, R. U.; da Rocha, A. F.; Cascão, C. A. Jr.; Borges, G. A.; Nascimento, F. A. O. & Veneziano, W. H. (2005), Reconhecimento de padrões de sinais de EMG para controle de prótese de perna, Proceedings XI Congresso Brasileiro de Biomecânica.

Fukuda, O.; Tsuji, T.; Kaneko, M. & Otsuka, A. (2003). A human-assisting manipulator teleoperated by EMG signals and arm motions, IEEE Trans. Rob. Autom., Vol. 19, pp. 210-22.

Gao, J. B. & Harris, C. J. (2002). Some remarks on Kalman filters for the multisensor fusion. Information Fusion, Vol. 3, pp. 191-201.

Grimes, D. L.; Flowers, W. C. & Donath, M. (1977). Feasibility of an active control scheme for above knee prostheses, Journal Biomechanical Engineering, Vol. 99, pp. 215-221.

Hagan, M. T. & Menhaj, M. B. (1994). Training feedforward networks with the Marquardt algorithm, IEEE Trans. Neural Networks, Vol. 5, pp. 989-93.

Hall, D. L. & Llinas, J. (1997). An introduction to multisensor data fusion, Proceedings IEEE, pp. 6-23.

Hargrove, L., Englehart, K. & Hudgins, B. (2008). A training strategy to reduce classification degradation due to electrode displacements in pattern recognition based myoelectric control, Biomed. Signal Process. Control, Vol. 3, pp. 175-80.

Haykin, S. (1999). Neural Networks: A Comprehensive Foundation, Prentice Hall 2nd edn, New Jersey.

Huang, Y.; Englehart, K.; Hudgins, B. & Chan, A. D. C. (2005). A Gaussian mixture model based classification scheme for myoelectric control of powered upper limb prostheses, IEEE Trans. Biomed. Eng, Vol. 52, pp. 1801-11.

Hudgins, B.; Parker, P. A. & Scott, R. N. (1993). A new strategy for multifunction myoelectric control, IEEE Trans. Biomedical Eng., Vol. 40, No. 1, pp. 82-94.

Ito, K.; Tsukamoto, M. & Kondo, T. (2008). Discrimination of intended movements based on nonstationary EMG for a prosthetic hand control, Proceedings the ISCCSP, pp. 14-19.

Ishihara, J.Y.; Terra, M.H.; Borges, G.A.; Scandaroli, G.G.; Inoue, R.S.; Grassi Jr., V. (2009). Applications of Robust Descriptor Kalman Filter in Robotics. In: Victor M. Moreno ; Alberto Pigazo. (Org.). Kalman Filter: Recent Advances and Applications. Vienna: I-Tech Education and Publishing KG, pp. 507-534.

Kang, W. J.; Shiu, J. R.; Cheng, C. K.; Lai, J. S. & Tsao, H. W. (1995). The Application of Cepstral Coefficients and Maximum Likelihood Method in EMG Pattern Recognition, IEEE

Transactions on Biomedical Engineering, Vol. 42, pp. 777-785.
Kastner, J.; Nimmervoll, R. & Wagner, I. P. (1999). What are the benefits of the Otto Bock C-leg? A comparative gait analysis of C-leg, 3R45 and 3R80, Journal Medical Orthopedic, Vol. 119, pp. 131-137.
Kelly, M. F.; Parker, P. A. & Scott, R. N. (1990). The application of neural networks to myoelectric signal analysis: a preliminary study, IEEE Trans. Biomed. Eng., Vol. 37, pp. 221-30.
Kohonen, T. (2001). Self-Organizing Maps, New York: Springer, 3rd edn.
Liu, Y. H.; Huang, H. P. & Weng, Ch. H. (2007). Recognition of electromyographic signals using cascade kernel learning machine, IEEE/ASME Trans. Mechatron, Vol. 12, pp. 253-64.
Ljung, L. (1987). System Identification: Theory for the User, Prentice Hall, New Jersey.
Lopez, N. M.; di Sciascio, F.; Soria, C. M. & Valentinuzzi, M. E. (2009). Robust EMG sensing system based on data fusion for myoelectric control of a robotic arm, Biomedical Engineering Online, Vol. 8, No. 5.
Luo, R. C. (1996). Sensor technologies and microsensor issues for mechatronics system, IEEE/ASME Trans. Mechatron, Vol. 1, pp. 39-49.
Luo, R. C.; Yih, Ch. & Su, K. L. (2002). Multisensor Fusion and Integration: Approaches, Applications, and Future Research Directions, IEEE Sensor, Vol. 2, pp. 107-119.
Manyika, J. & Durrant-Whyte, H. (1994). Data Fusion and Sensor Management:A Descentralized Information – Theoretic Approach, Ellis Horwood, London.
Merletti, R. & Parker, P. (2004). Electromyography: Engineering and Noninvasive Applications, John Wiley & Sons - IEEE Press, ISBN 978-0-471-67580-8, Hoboken, NJ, USA.
Oskoei, M. A. & Hu, H. (2007). Myoelectric Control System - A survey. Biomedical Signal Processing and Control, Vol. 2, pp. 275-294.
Parker, P.; Englehart, K. & Hudgins, B. (2006). Myoelectric signal processing for control of powered limb prostheses, Journal of Electromyography and Kinesiology, Vol. 16, pp. 541-548.
Popovic, D.; Oguztorelli, M. N. & Stein, R. B. (1995). Optimal control for an above-knee prosthesis with two degrees of freedom, Journal of Biomechanics, Vol. 28, pp. 89-98.
Rodrigues, S. S.; Ferreira, R. U.; Marques Junior, M. F.; Beckmann, E. D.; Santos, G. F.; Borges, G. A.; Ishihara, J. Y. & da Rocha, A. F. (2006). Estudo e desenvolvimento de uma prótese robótica de perna comandada por sinais eletromiográficos. Proceedings IV Congresso Ibero-Americano Sobre Tecnologias de Apoio a Portadores de Deficiência.
SENIAM (2008). Surface Electromyography for Noninvasive Assessment of muscle, [http://www.seniam.org].
Silva, J.; Chau, T. & Goldenberg, A. (2003). MMG-Based Multisensor Data Fusion for Prosthesis Control. Proceedings IEEE CMBS, pp. 2909-2912.
Smith, R. J.; Tenore, F.; Huberdeau, D.; Etiene-Cummings, R. & Thakor, N. V. (2008). Continuous decoding of finger position from surface EMG signals for the control of powered prostheses, Proceedings of the 2008 IEEE/EMBC 30th Annual International Conference Engineering in Medicine and Biology Society, pp. 2393-2396.
Sommerich, C. M.; Joines, S. M., Hermans, V. & Moon, S. D. (2000). Use of surface electromyography to estimate neck muscle activity, J. Electromyography Kinesiol., No. 6, pp. 377-98.
Vaseghi, S. V. (2000). Advanced Digital Signal Processing and Noise Reduction, John Wiley

Publisher, 2nd edn, New York.

Wang, G.; Wang, Z.; Chen, W. & Zhuang, J. (2006). Classification of surface EMG signals using optimal wavelet packet method based on Davies-Bouldin criterion, Med. Biol. Eng. Comput., Vol. 44, pp. 865-72.

Zardoshti-Kermani, M.; Wheeler, B. C.; Badie, K. & Hashemi, R. M. (1995). EMG feature evaluation for movement control of upper extremity prosthesis, IEEE Trans. Rehabil. Eng., Vol. 3, pp. 324-33.

Zhao, J.; Xie, Z.; Jiang, L.; Cai, H.; Lio, H. & Hirzinger, G. (2006). EMG control for a five-fingered interactuated prosthetic hand based on wavelet transform and sample entropy, Proceedings IEEE/RSJ Int. Conf. Intelligent Robots and Systems, pp. 3215-20.